

Anisotropic Elastic Properties of CeRhIn₅

Ravhi S. Kumar, H. Kohlmann, B.E. Light, and A.L. Cornelius
Department of Physics, University of Nevada, Las Vegas, Nevada, 89154-4002

V. Raghavan, T.W. Darling, J.L. Sarrao
Materials Science and Technology Division, Los Alamos National Laboratory, Los Alamos, NM 87545
(Date textdate)

The structure of the quasi two dimensional heavy fermion antiferromagnet CeRhIn₅ has been investigated as a function of pressure up to 13 GPa using a diamond anvil cell under both hydrostatic and quasihydrostatic conditions at room ($T = 295$ K) and low ($T = 10$ K) temperatures. Complementary resonant ultrasound measurements were performed to obtain the complete elastic moduli. The bulk modulus ($B \approx 78$ GPa) and uniaxial compressibilities ($\kappa_a = 3.96 \times 10^{-3}$ GPa⁻¹ and $\kappa_c = 4.22 \times 10^{-3}$ GPa⁻¹) found from pressure-dependent x-ray diffraction are in good agreement with the ultrasound measurements. Unlike doping on the Rh site where T_c increases linearly with the ratio of the tetragonal lattice parameters c/a , no such correlation is observed under pressure; instead, a double peaked structure with a local minimum around 4-5 GPa is observed at both room and low temperatures.

PACS numbers: 61.10.Nz, 62.50.+p, 51.35.+a, 71.27.+a, 74.70.Tx

I. INTRODUCTION

Ce based heavy fermion (HF) antiferromagnetic (AF) compounds have been the subject of intensive investigations due to their unconventional magnetic and superconducting properties. In these compounds the electronic correlations, the magnetic ordering temperature and the crystal field effects are sensitive to pressure, and pressure induced superconductivity has been observed in a variety of compounds such as CePd₂Si₂, CeCu₂Ge₂, CeRh₂Si₂ and CeIn₃^{1,2,3,4,5,6}. The appearance of superconductivity in these systems and the deviation from Fermi liquid behavior as a function of pressure are still challenging problems to be studied. Recently, HF systems with the formula CeMIn₅ ($M = \text{Co}$ and Ir) have been reported to become superconductors at ambient pressure^{7,8}, while CeRhIn₅ is an antiferromagnet at ambient pressure ($T_N = 3.8$ K and $\gamma \approx 400$ mJ/mol K²). These compounds crystallize in the HoCoGa₅ structure with alternating stacks of CeIn₃ and MIn₂ along the c axis. Thermodynamic⁹, NQR¹⁰, and neutron scattering¹¹ experiments all show that the electronic and magnetic properties of CeRhIn₅ are anisotropic in nature. The AF ordering in CeRhIn₅ is suppressed with applied pressure and superconductivity is observed at 1.6 GPa with $T_c = 2.1$ K. Like CeIn₃ the bulk nature of the SC state in CeRhIn₅ has been unambiguously established under pressure. The AF state is suppressed at a pressure of around 1.2 GPa and coexists over a limited pressure range with the superconducting (SC) state^{6,12,13}.

The value of T_c in magnetically mediated superconductors is believed to be dependent on dimensionality in addition to the characteristic spin fluctuation temperature. Theoretical models and experimental results suggest that SC state in CeRhIn₅ may be due to the quasi-two dimensional (2D) structure and anisotropic AF fluctuations which are responsible for the enhancement of T_c

relative to CeIn₃^{14,15}. A strong correlation between the ambient pressure c/a ratio and T_c in the CeMIn₅ compounds is indicative of the enhancement of the superconducting properties by lowering dimensionality (increasing c/a increases T_c)¹⁴. In order to explain the evolution of superconductivity induced by pressure and the suppression of AF ordering, it is important to probe the effect of pressure on structure for this compound and look for possible correlations between structural and thermodynamic properties.

Here we report on high pressure x-ray diffraction measurements performed on CeRhIn₅ up to 13 GPa at high ($T = 295$ K) and low ($T = 10$ K) temperatures under both hydrostatic and quasihydrostatic conditions. As the measured linear compressibilities are similar for both the a and c directions, the results for all pressure measurements, both hydrostatic and quasihydrostatic, are similar. The elastic properties obtained from the high pressure measurements are compared to the full set of elastic constants obtained from resonant ultrasound (RUS) measurements, and excellent agreement is found in the measured bulk modulus ($B \approx 78$ GPa) from both techniques. We find no direct correlation between c/a and T_c as a function of pressure. Rather, a double peaked structure with a local minimum around 4-5 GPa is observed for c/a at both room and low temperatures.

II. EXPERIMENT

CeRhIn₅ single crystals were grown by a self flux technique¹⁶. The single crystals were crushed into powder and x-ray diffraction measurements show the single phase nature of the compound. In agreement with previous results¹⁶, the crystals were found to have tetragonal symmetry with cell parameters $a = 4.6531(1)$ Å, $c = 7.538(9)$ Å.

The high pressure x-ray diffraction (XRD) experiments were performed using a rotating anode x-ray generator (Rigaku) for Runs 1-4 ($\lambda = 0.7093 \text{ \AA}$) and synchrotron x-rays at HPCAT ($\lambda = 0.4218 \text{ \AA}$), Sector 16 at the Advanced Photon Source for Run 5 and the low temperature measurement. The sample was loaded with NaCl or MgO powder as a pressure calibrant and either a 4:1 Methanol ethanol mixture (hydrostatic) or NaCl (quasi-hydrostatic) as the pressure transmitting medium in a Re gasket with a $180 \mu\text{m}$ diameter hole. High pressure was achieved using a Merrill-Basset diamond anvil cell with $600 \mu\text{m}$ culet diameters. The XRD patterns are collected using an imaging plate ($300 \times 300 \text{ mm}^2$) camera with $100 \times 100 \mu\text{m}^2$ pixel dimensions. XRD patterns were collected up to 13 GPa at room ($T = 295 \text{ K}$) and low (down to $T = 10 \text{ K}$) temperatures. The low temperature measurements were made in a continuous flow cryostat. The images were integrated using FIT2D software¹⁷. The structural refinement of the patterns was carried out using the Rietveld method on employing the FULLPROF and REITICA (LHPM) software packages¹⁸. The RUS technique is described in detail elsewhere^{19,20}.

By measuring the resonant frequencies of a well aligned single crystal of CeRhIn_5 , we can determine the full set of room temperature elastic constants. This will give the adiabatic bulk modulus B^S rather than the isothermal bulk modulus B_0 found in the pressure measurements.

III. RESULTS AND DISCUSSION

In Fig. 1 we show the XRD patterns for CeRhIn_5 obtained at two different quasi-hydrostatic pressures with NaCl used as the pressure transmitting media. The raw data (crosses), Rietveld fit to the data (solid line through the data points), fit reflections (vertical lines) and the difference between the fit and experiment (solid line near bottom) are all shown. Fig. 2 shows the diffraction data at five different pressures. Diffraction peaks from the Re gasket (labeled g), NaCl (labeled *) and CeRhIn_5 (no label) are all observed in Fig. 2. The known equation of state for NaCl²¹ or the standard ruby fluorescence technique²² was used to determine the pressure. The refinement of the CeRhIn_5 XRD patterns was performed on the basis of the $P4/mmm$ space group (No. 123). The HoCoGa_5 structure in which CeRhIn_5 crystallizes contains layers of cubo-octohedra of the structural type of AuCu_3 and layers of PtHg_2 structure type. The unit cell consists of Ce atoms situated at the corners and In atoms at two inequivalent sites. In1 is surrounded by Ce and located at the top and bottom faces while In2 is stacked between Ce-In and Rh layers. The hybrid structure is related to both CeIn_3 and Ce_2RhIn_8 . When comparing the crystallographic data and bulk modulus of CeIn_3 it is evident that the Ce atom in CeRhIn_5 experiences a chemical pressure of 1.4 GPa at ambient conditions^{6,9}.

The results of the Rietveld refinement at different pressures have been listed in Table I.

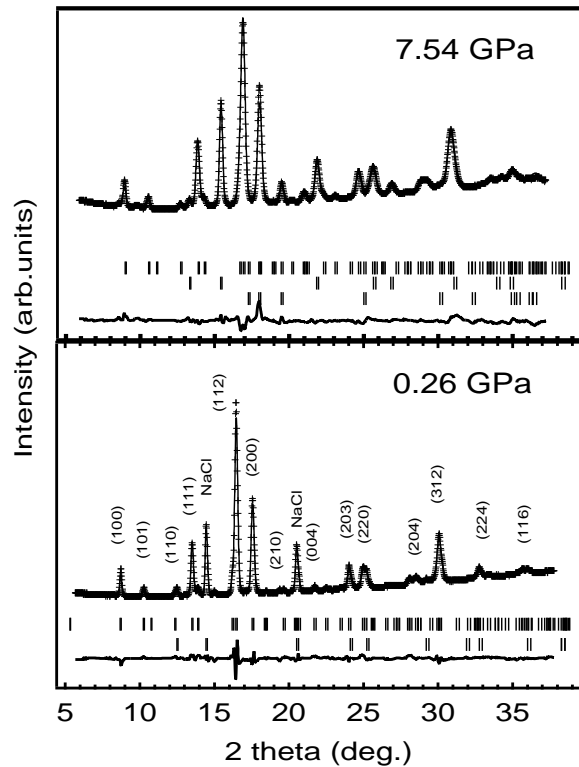


FIG. 1: Rietveld refinements for the high pressure x-ray diffraction patterns of CeRhIn_5 at 0.26 GPa and 7.54 GPa. The NaCl pressure marker and various reflections from CeRhIn_5 are labeled.

	1.47 GPa	3.97 GPa	5.18 GPa	7.54 GPa
$a(\text{\AA})$	4.6263(3)	4.5718(3)	4.5712(3)	4.5298(3)
$c(\text{\AA})$	7.505(1)	7.409(1)	7.396(1)	7.337(1)
In2 (z)	0.3036(3)	0.3049(4)	0.3089(3)	0.3058(3)
$B_{\text{Ce}}(\text{\AA}^2)$	0.3(1)	0.5(2)	0.3(1)	0.5(1)
$B_{\text{Rh}}(\text{\AA}^2)$	0.9(1)	1.3(3)	1.0(2)	1.7(1)
$B_{\text{In1}}(\text{\AA}^2)$	1.7(2)	3.8(4)	1.4(3)	1.4(2)
$B_{\text{In2}}(\text{\AA}^2)$	1.4(1)	1.3(1)	1.2(1)	0.80(7)
R_p (%)	2.1	2.6	2.5	2.1
R_{wp} (%)	3.0	3.8	3.5	3.0

TABLE I: Room temperature structural parameters, isotropic thermal parameters B , and R factors of CeRhIn_5 at different pressures. The crystal structure is tetragonal and space group symmetry is $P4/mmm$ (No.123) with $Z = 1$. The atomic sites are Ce at 1a [0, 0, 0], Rh at 1b [0, 0, 0.5], In1 at 1c [0.5, 0.5, 0] and In2 at 4i [0, 0.5, z].

During the refinement, a total of nineteen parameters have been optimized which include the background, scale factors, lattice parameters, profile parameters, temperature factors, zero point shift parameter and atomic coordinate. Initially the refinement has been started for two phases in most cases including the pressure calibrant, and at higher pressures an additional phase for the gasket has been added. At higher pressures, considerable changes in the isotropic temperature factors are observed for In1,

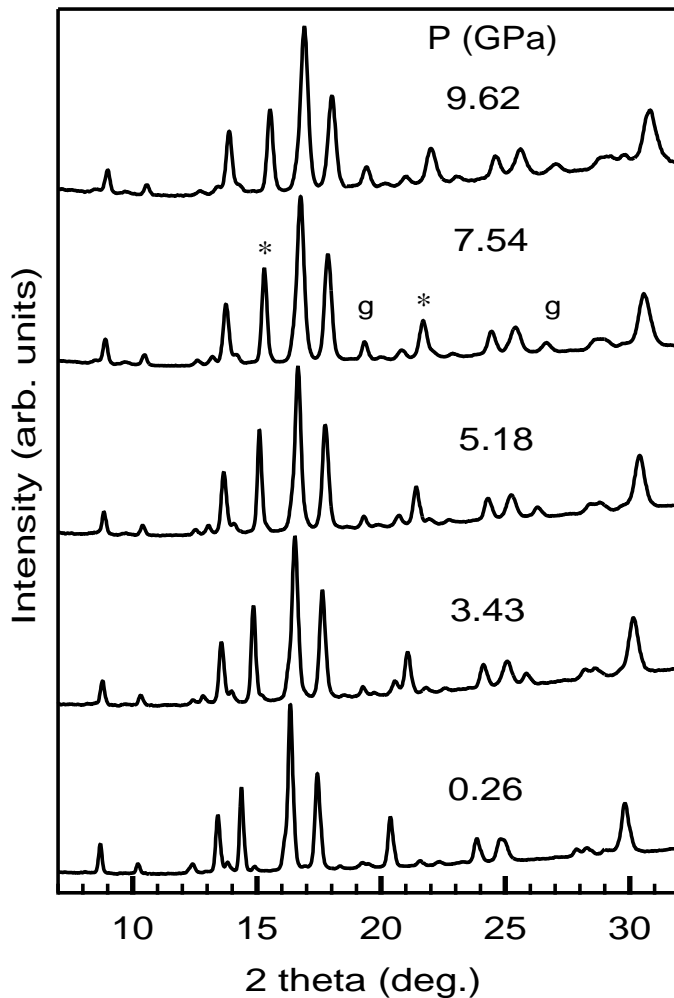


FIG. 2: X-ray diffraction patterns collected at various pressures for CeRhIn_5 . Peaks labeled (g) correspond to the Re gasket and (*) to the NaCl pressure marker. Peaks without a label are from the CeRhIn_5 sample.

In2 and Rh during the refinement.

The $V(P)$ data has been plotted for CeRhIn_5 for quasi-hydrostatic (Run 1 and Run 2) and hydrostatic (Runs 3-5) measurements in Fig. 3. Since the maximum volume compression is only of the order of 10%, the $V(P)$ data has been fit using a least squares fitting procedure to the second order Murnaghan equation of state

$$P = \frac{B_0}{B'_0} \left[\left(\frac{V_0}{V(P)} \right)^{B'_0} - 1 \right]. \quad (1)$$

For the room temperature ($T = 295$ K) data in Fig. 3, we find $B_0 = 78.4 \pm 2.0$ GPa and $B'_0 = 5.6 \pm 0.6$. The RhIn_2 layers in CeRhIn_5 appear to stiffen the structure relative to CeIn_3 which has a smaller bulk modulus ($B = 67$ GPa)²³. The bulk modulus value compares well with the values reported for other HF systems^{24,25,26,27}. Fig. 3 also shows the ratio of the lattice constants c/a as a function of pressure. For all of the measurements,

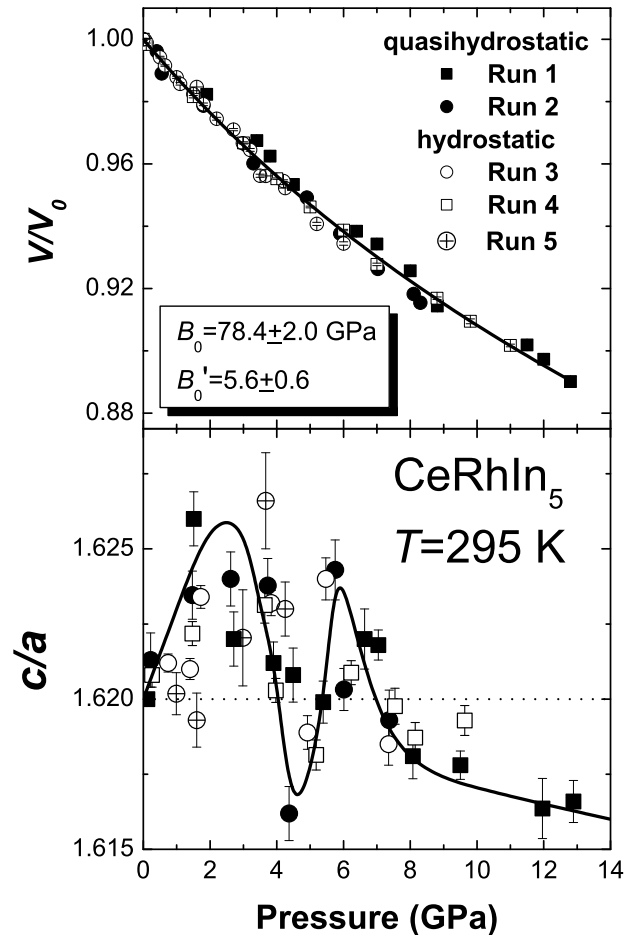


FIG. 3: Normalized volume V/V_0 and ratio of tetragonal lattice constants c/a plotted versus pressure for CeRhIn_5 at room temperature. Five separate runs, two quasi-hydrostatic (filled symbols) and three hydrostatic (open symbols) are displayed. The solid line through the volume data is a fit to all of the data using $B_0 = 78.4$ GPa and $B'_0 = 5.6$. The dashed line shows the ambient pressure c/a value. The line through the c/a data is a guide for the eye.

there appears to be a double peak structure with a local minimum around 4-5 GPa. Note that the isotropic thermal parameters for the In sites, in particular the In1 site, have their largest values around 4 GPa. The initial values of the linear compressibilities (average values from the hydrostatic measurements for $P < 2$ GPa) are $\kappa_a = (3.96 \pm 0.08) \times 10^{-3}$ GPa⁻¹ and $\kappa_c = (4.22 \pm 0.10) \times 10^{-3}$ GPa⁻¹. The similarity between the measured values of κ_a and κ_b are likely the reason that no discernible difference is found for the hydrostatic and quasi-hydrostatic cases. The $P - V$ data shows that the system retains its crystal structure up to the pressure limit (13 GPa) investigated.

We have also investigated the $V(P)$ behavior at low temperature ($T = 10$ K). As the superconducting transition has a maximum around 2 K, it is desirable to obtain structural data in the low temperature regime when try-

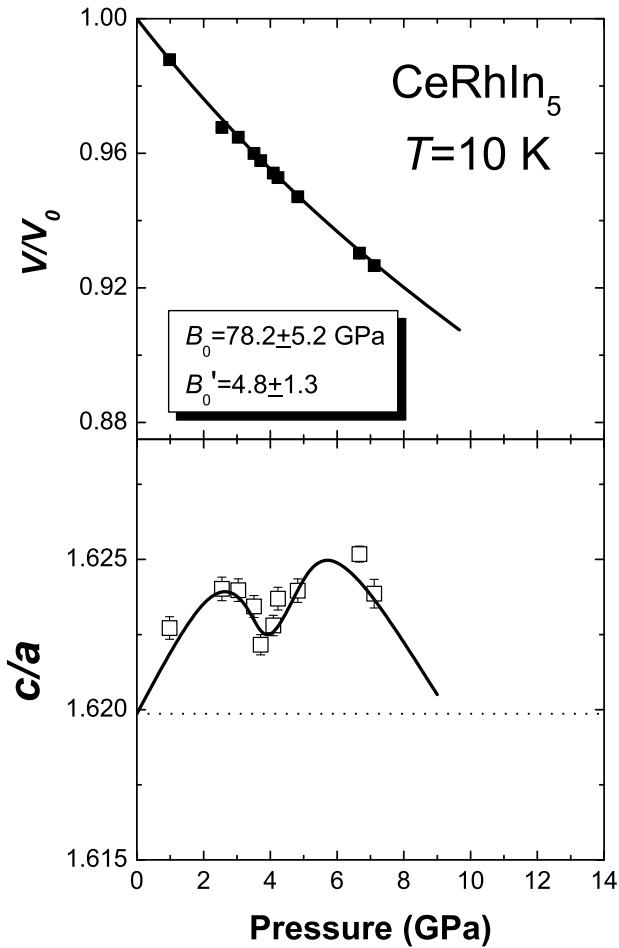


FIG. 4: Normalized volume V/V_0 and ratio of tetragonal lattice constants c/a plotted versus pressure for CeRhIn_5 at 10 K. The solid line through the volume data is a fit to all of the data using $B_0 = 78.2 \pm 5.2$ GPa and $B'_0 = 4.8$. The dashed line shows the ambient pressure c/a value. The solid line through the c/a data is a guide for the eye.

ing to correlate superconductivity to structural measurements. The results for a single hydrostatic measurement at 10 K is shown in Fig. 4. The value of $B_0 = 78.2 \pm 5.2$ GPa is identical to the room temperature value within the experimental uncertainty. Though the lattice does contract at ambient pressure as temperature is lowered which would lead to a higher bulk modulus, the expected change is within our experimental uncertainty. The variation of c/a as a function of pressure again shows a double maximum structure at low temperature in a manner similar to the room temperature data.

As mentioned, a strong correlation between the ambient pressure c/a ratio and T_c in the CeMIn_5 compounds has been observed (increasing c/a increases T_c)¹⁴. To further investigate the variation of c/a with pressure and temperature, we plot the value of c/a as a function of temperature at $P = 6.9$ GPa in Fig. 5. As can be seen, there is a significant enhancement of c/a at 6.9 GPa relative to the ambient pressure thermal expansion data of

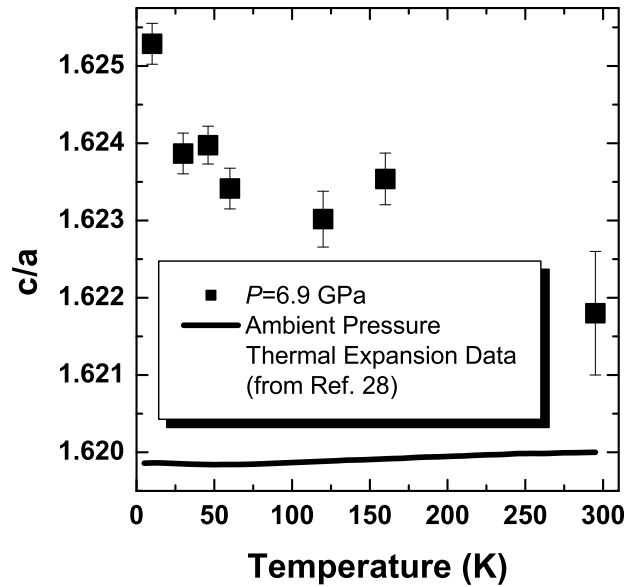


FIG. 5: Ratio of tetragonal lattice constants c/a plotted versus temperature for CeRhIn_5 at $P = 6.9$ GPa. The solid line is from ambient pressure thermal expansion data (Ref. 28).

Takeuchi *et al.*²⁸ Unlike the ambient pressure data, c/a appears to increase as temperature is lowered at 6.9 GPa. Taken as a whole, the current results seem to show no direct correlation between the values of c/a and T_c under pressure. However, the value of c/a (≈ 1.624) where $T_c(P)$ has its maximum around 2.5 GPa is consistent with a correlation between the room temperature value of c/a and T_c for various CeMIn_5 compounds.¹⁴ This leads to the natural conclusion that hybridization effects are likely the driving force behind the observed $T_c(P)$ behavior in CeRhIn_5 . We will discuss this in further detail later.

The complete set of elastic constants were measured using the RUS technique and the results are shown in Table II. The values of the adiabatic compressibility B^S , tetragonal shear modulus C^t , and linear compressibilities (κ_a, κ_c) can be calculated from the measured elastic constants²⁹ and are given by

$$B^S = \frac{C_{33}(C_{11} + C_{12}) - 2C_{13}^2}{2C_{33} + C_{11} + C_{12} - 4C_{13}} \quad (2)$$

and

$$C^t = \frac{1}{6} (2C_{33} + C_{11} + C_{12} - 4C_{13}). \quad (3)$$

The results are displayed in Table II. The value of B^S is slightly larger than the isothermal value B_0 obtained from the pressure measurements. This is to be expected as the ratio $B^S/B_0 = 1 + \beta\gamma_{th}T$, where $\beta = 4.6 \times 10^{-5} \text{ K}^{-1}$ is the volume thermal expansion coefficient²⁸ and γ_{th} is the thermal Gruneisen parameter which is typically of the order of unity. At room temperature then, one

Elastic Constant	Value (GPa)
C_{11}	146.7
C_{12}	45.8
C_{44}	43.4
C_{33}	141.4
C_{13}	54.0
C_{66}	41.8
Moduli	Value (GPa)
B^S (RUS)	82.5
C^t (RUS)	43.2
B_0 (P)	78.4
Compressibilities	Value (GPa $^{-1}$)
κ_a (RUS)	4.09×10^{-3}
κ_c (RUS)	3.96×10^{-3}
κ_a (P)	3.96×10^{-3}
κ_c (P)	4.22×10^{-3}

TABLE II: A summary of the CeRhIn₅ elastic constants C_{ij} measured using resonant ultrasound and the various moduli and compressibilities measured by resonant ultrasound (RUS) and pressure (P).

then expects $B^S/B_0 \approx 1.01 - 1.02$ which is in reasonable agreement with our experimental value of 1.05 ± 0.03 .

In all of the measurements, the c/a ratio is found to have a double peaked structure. As mentioned previously, the hybridization between the Ce 4f electrons and the conduction electrons should mainly depend on the distance between Ce and its nearest neighbors. In fact, a simple model to estimate the hybridization by means of a tight-binding calculation shows that the hybridization should have the relatively strong d^{-6} dependence for hybridization between f and d electrons, where d is the distance between the atoms containing the d and f electrons (in our case, this would be Rh and Ce respectively)^{30,31}.

To examine the pressure dependence of d , the Ce-In1 and Ce-In2 bond lengths are plotted in Fig. 6 for the hydrostatic measurements. The Ce-In1 bond is less compressible than the Ce-In2 bond. The Ce-In2 data appears to display plateaus between 0-2 and 3-5 GPa. The structural results may be compared with the high pressure resistivity experimental data reported for CeRhIn₅^{6,32}. First, the temperature corresponding to the maximum in the resistivity, often taken to be a measure of the Kondo temperature T_K is seen to initially decrease in CeRhIn₅ in contrast to the usually observed behavior³³. One possible explanation for this effect could lie in an initial increase in the Ce-In2 bond length causing an anomalous initial decrease in the hybridization. Whereas the plot of Ce-In1 bond length with pressure shows a gradual decrease with increasing pressure. Our data is not sufficient to make any definite conclusions along these lines. The smooth decrease in the Ce-In1 bond length would lead one to expect the typical inverse parabolic $T_c(P)$ dependence consistent with theoretical calculations¹⁵, measurements on CeRhIn₅^{6,32} and most heavy fermion superconductors^{3,4,5}.

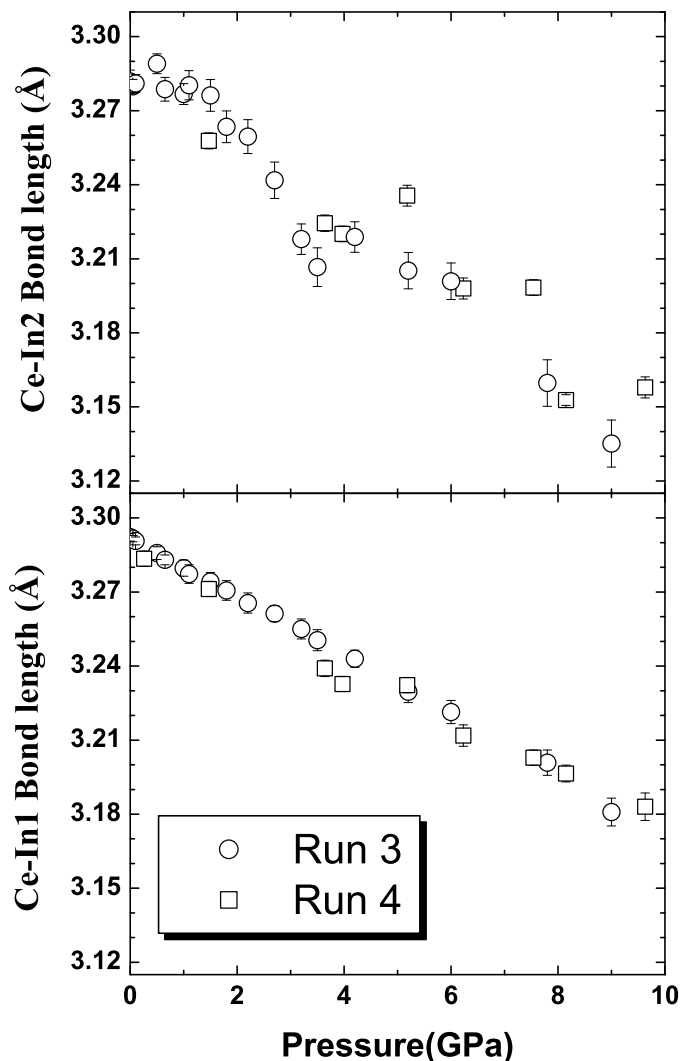


FIG. 6: The measured Ce-In1 and Ce-In2 bond lengths for both hydrostatic measurements on CeRhIn₅ as a function of pressure.

IV. CONCLUSIONS

We have studied the elastic properties of the heavy fermion system CeRhIn₅ using resonant ultrasound and hydrostatic and quasihydrostatic pressures up to 13 GPa using x-ray diffraction. The bulk modulus ($B = 78$ GPa) and uniaxial compressibilities ($\kappa_a = 3.96 \times 10^{-3}$ GPa $^{-1}$ and $\kappa_c = 4.22 \times 10^{-3}$ GPa $^{-1}$) found from pressure-dependent x-ray diffraction are in good agreement with the ultrasound measurements. Unlike doping experiments which hint at a strong correlation between the c/a ratio and T_c , pressure shows no such correlation as a double peaked structure with a local minimum around 4-5 GPa is found at 295 K and 10 K.

Acknowledgments

We thank Maddury Somayazulu, Beam Line Scientist at HPCAT for assistance on the low temperature, high pressure diffraction measurements. Work at UNLV is supported by DOE EPSCoR-State/National Laboratory Partnership Award DE-FG02-00ER45835. Work at LANL is performed under the auspices of the U.S. Department of Energy. HPCAT is a collaboration among the UNLV High Pressure Science and Engineering Cen-

ter, the Lawrence Livermore National Laboratory, the Geophysical Laboratory of the Carnegie Institution of Washington, and the University of Hawaii at Manoa. The UNLV High Pressure Science and Engineering Center was supported by the U.S. Department of Energy, National Nuclear Security Administration, under Cooperative Agreement DE-FC08-01NV14049. Use of the Advanced Photon Source was supported by the U. S. Department of Energy, Office of Science, Office of Basic Energy Sciences, under Contract No. W-31-109-Eng-38.

-
- ¹ F. Steglich, J. Aarts, C. D. Bredl, W. Lieke, D. Meschede, W. Franz, and H. Schäfer, *Phys. Rev. Lett.* **43**, 1892 (1979).
- ² D. Jaccard, K. Behina, and J. Sierro, *Phys. Lett. A* **163**, 475 (1992).
- ³ R. Movshovich, T. Graf, D. Mandrus, J. D. Thompson, J. L. Smith, and Z. Fisk, *Phys. Rev. B* **53**, 8241 (1996).
- ⁴ F. M. Grosche, S. R. Julian, N. D. Mathur, and G. G. Lonzarich, *Physica B* **223-224**, 50 (1996).
- ⁵ N. D. Mathur, F. M. Grosche, S. R. Julian, I. R. Walker, D. M. Freye, R. K. Haselwimmer, and G. G. Lonzarich, *Nature* **394**, 39 (1998).
- ⁶ H. Hegger, C. Petrovic, E. G. Moshopoulou, M. F. Hundley, J. L. Sarrao, Z. Fisk, and J. D. Thompson, *Phys. Rev. Lett.* **84**, 4986 (2000).
- ⁷ C. Petrovic, P. G. Pagliuso, M. F. Hundley, R. Movshovich, J. L. Sarrao, J. D. Thompson, Z. Fisk, and P. Monthoux, *J. Phys.:Condens. Matter* **13**, L337 (2001).
- ⁸ C. Petrovic, R. Movshovich, M. Jaime, P. G. Pagliuso, M. F. Hundley, J. L. Sarrao, Z. Fisk, and J. D. Thompson, *Europhys. Lett.* **53**, 354 (2001).
- ⁹ A. L. Cornelius, A. J. Arko, J. L. Sarrao, M. F. Hundley, and Z. Fisk, *Phys. Rev. B* **62**, 14181 (2000).
- ¹⁰ N. J. Curro, P. C. Hammel, P. G. Pagliuso, J. L. Sarrao, J. D. Thompson, and Z. Fisk, *Phys. Rev. B* **62**, R6100 (2000).
- ¹¹ W. Bao, P. G. Pagliuso, J. L. Sarrao, J. D. Thompson, Z. Fisk, J. W. Lynn, and R. W. Erwin, *Phys. Rev. B* **62**, R14621 (2000).
- ¹² R. A. Fisher, F. Bouquet, N. E. Phillips, M. F. Hundley, P. G. Pagliuso, J. L. Sarrao, Z. Fisk, and J. D. Thompson, *Phys. Rev. B* **65**, 224509 (2002).
- ¹³ T. Mito, S. Kawasaki, G. q. Zheng, Y. Kawasaki, K. Ishida, Y. Kitaoka, D. Aoki, Y. Haga, and Y. Onuki, *Phys. Rev. B* **63**, 220507(R) (2001).
- ¹⁴ P. G. Pagliuso, R. Movshovich, A. D. Bianchi, M. Nicklas, N. O. Moreno, J. D. Thompson, M. F. Hundley, J. L. Sarrao, and Z. Fisk, *Physica B* **312-313**, 129 (2002).
- ¹⁵ P. Monthoux and G. G. Lonzarich, *Phys. Rev. B* **63**, 054529 (2001).
- ¹⁶ E. G. Moshopoulou, Z. Fisk, J. L. Sarrao, and J. D. Thompson, *J. Solid State Chem.* **158**, 25 (2001).
- ¹⁷ A. P. Hammersley, S. O. Svensson, M. Hanfland, A. N. Fitch, and D. Häusermann, *High Pressure Research* **14**, 235 (1996).
- ¹⁸ J. Rodriguez-Carvajal, *Physica B* **192**, 55 (1993).
- ¹⁹ A. Migliori, J. L. Sarrao, W. M. Visscher, T. M. Bell, M. Lei, Z. Fisk, and R. G. Leisure, *Physica B* **183**, 1 (1993).
- ²⁰ A. Migliori and J. L. Sarrao, *Resonant Ultrasound Spectroscopy* (John Wiley and Sons, Inc., New York, 1997).
- ²¹ J. M. Brown, *J. Appl. Phys.* **86**, 5801 (1999).
- ²² G. J. Piermarini, S. Block, J. D. Barnett, and R. A. Forman, *J. Appl. Phys.* **46**, 2774 (1975).
- ²³ I. Vedel, A. M. Redon, J. M. Mignot, and J. M. Leger, *J. Phys. F: Metal Phys.* **17**, 849 (1987).
- ²⁴ T. Penney, B. Barbara, T. S. Plaskett, H. E. J. King, and S. J. LaPlaca, *Solid State Commun.* **44**, 1199 (1982).
- ²⁵ I. L. Spain, F. Steglich, U. Rauchschwalbe, and H. D. Hochheimer, *Physica B* **139-140**, 449 (1986).
- ²⁶ A. P. G. Kutty and S. N. Vaidya, in *Theoretical and Experimental Aspect of Valence Fluctuations and Heavy Fermions*, edited by L. C. Gupta and S. K. Malik (Plenum, New York, 1987), p. 621.
- ²⁷ C. Wassilew-Reul, M. Kunz, M. Hanfland, D. Häusermann, C. Geibel, and F. Steglich, *Phys. Rev. B* **230-232**, 310 (1997).
- ²⁸ T. Takeuchi, T. Inoue, K. Sugiyama, D. Aoki, Y. Tokiwa, Y. Haga, K. Kindo, and Y. Onuki, *J. Phys. Soc. Jpn.* **70**, 877 (2001).
- ²⁹ J. C. Boettger, *Phys. Rev. B* **55**, 750 (1997).
- ³⁰ W. A. Harrison, *Phys. Rev. B* **28**, 550 (1983).
- ³¹ T. Endstra, G. J. Nieuwenhuys, and J. A. Mydosh, *Phys. Rev. B* **48**, 9595 (1993).
- ³² T. Muramatsu, N. Tateiwa, T. C. Kobayashi, A. Shimizu, K. Amaya, D. Aoki, H. Shishido, Y. Haga, and Y. Onuki, *J. Phys. Soc. Jpn.* **70**, 3362 (2001).
- ³³ J. D. Thompson, *Physica B* **190**, 61 (1993).